GEOPHYSICAL RESEARCH LETTERS, VOL. 40, 1–6, doi:10.1002/2013GL057680, 2013

Sn propagation in the Western United States from common midpoint stacks of USArray data

J. S. Buehler[1] and P. M. Shearer[1]

Received 14 August 2013; revised 19 November 2013; accepted 22 November 2013.

[1] The regional seismic phase *Sn* propagates horizontally in the uppermost mantle and is sensitive to lateral variations in mantle lid thickness, temperature, and melt. *Sn* is therefore often used as an indicator for physical properties of the lithosphere. It has previously been noticed that *Sn* is not observed at many stations in the Western United States and *Sn* seems especially highly attenuated for paths across the Basin and Range. Here we apply stacking methods to USArray data to identify highly attenuating regions in the uppermost mantle and increase the spatial resolution of the *Sn* propagation image. We find evidence for *Sn* propagation at short ranges in the central Great Basin and the northeastern part of the Colorado Plateau, both regions where lithospheric stability and thickness is debated, and observe strong *Sn* attenuation around the perimeter of the central Great Basin. **Citation:** Buehler, J. S., and P. M. Shearer (2013), *Sn* propagation in the Western United States from common midpoint stacks of USArray data, *Geophys. Res. Lett.*, *40*, doi:10.1002/2013GL057680.

1. Introduction

[2] We investigate high-frequency propagation of the regional phase *Sn* in the Western United States. *Sn* propagates horizontally in the uppermost mantle just below the Moho and is often modeled as a head wave. *Sn* has been used for velocity and attenuation studies focused on the uppermost mantle [e.g., *Diaz et al.*, 2013; *Goek et al.*, 2003; *Pei et al.*, 2007]. However, *Sn* has been observed to travel to teleseismic distances across oceanic paths and is more broadly defined as a channel wave that travels in the mantle lid above the low-velocity zone of the upper mantle [*Molnar and Oliver*, 1969; *Stephens and Isacks*, 1977]. A waveguide can be formed if the shear wave velocity increases with depth from the Moho to the top of the low-velocity zone. Several factors influence the propagation of *Sn*, not only the upper mantle shear wave velocity gradient [*Stephens and Isacks*, 1977] but also the thickness and thermal state of the lithosphere [*Beghoul et al.*, 1993]. Therefore, studies of *Sn* propagation can be used to help constrain regional tectonic models [e.g., *Barron and Priestley*, 2009; *Beghoul et al.*, 1993; *Calvert et al.*, 2000; *Ni and Barazangi*, 1983].

[3] Starting with the USArray station deployment, great efforts have been made to investigate and image lithospheric structure below the Western United States with various data sets and new methods to better understand the tectonic evolution of the continent. Tomographic images from body and surface wave data show very heterogeneous velocity structure in the upper mantle in the Western United States [e.g., *Lin et al.*, 2011; *Obrebski et al.*, 2011; *Schmandt and Humphreys*, 2010]. Prominent local low-velocity anomalies imaged below the Snake River Plain and the southwestern Colorado Plateau likely reflect higher temperatures due to volcanism. Waves that travel horizontally in the uppermost mantle will be strongly affected by these lateral anomalies. Higher temperatures should also increase seismic attenuation, which will affect *Sn* more than the *P* wave analog, *Pn*, as *S* wave mantle attenuation is observed to be stronger than *P* wave attenuation. Generally, *Sn* traverses well through stable continental regions but is attenuated in more tectonically active regions and *Beghoul et al.* [1993] concluded in their study on regional phase propagation that *Sn* does not propagate across the majority of the Western United States. However, *Beghoul et al.* [1993] also did not observe *Sn* for paths that cross below the relatively stable Colorado Plateau (Figure 1).

[4] In regions where the mantle lid is thin or missing, as for example through delamination processes that cause local upwelling of the asthenosphere, a process that may explain the elevation of the Colorado Plateau [e.g., *Levander et al.*, 2011], *Sn* will be strongly attenuated by the hotter material. Studies showed that the lithosphere is relatively thin for large portions of the Western United States: *Goes and van der Lee* [2002] estimated the lithosphere to be as thin as 50 km below the Basin and Range Province. *Beghoul et al*. [1993] estimated the mantle lid thickness to be about 20–40 km below the same region (adding a 20–30 km thick crust to compare to lithospheric thickness) and found no evidence for *Sn* in seismograms for paths that cross the Great Basin. However, more recent tomographic studies that profit from the USArray station network show finer-scale structure and possible drip features in the Great Basin that could locally increase lithospheric thickness [*West et al.*, 2009].

[5] In this study we use the dense USArray transportable network to investigate the propagation of the *Sn* phase. Previous research showed that at large scales *Sn* is strongly attenuated in regions west of the Great Plains [*Beghoul et al.*, 1993] (Figure 1). However, we find that there are a number of *Sn* picks in the database of the Array Network Facility (ANF) for stations west of the Great Plains, and an initial time term analysis with these picks showed that they are viable for tomography, as they produce similar large-scale features as *Pn* tomography maps. Many of these *Sn* picks have relatively short epicentral distances (< 6°), suggesting

Additional supporting information may be found in the online version of this article.

[1]Scripps Institution of Oceanography, University of California, San Diego, La Jolla, California, USA.

Corresponding author: J. S. Buehler, Scripps Institution of Oceanography, University of California, San Diego, La Jolla, CA 92093-0225, USA. (jsbuehle@ucsd.edu)

0094-8276/13/10.1002/2013GL057680

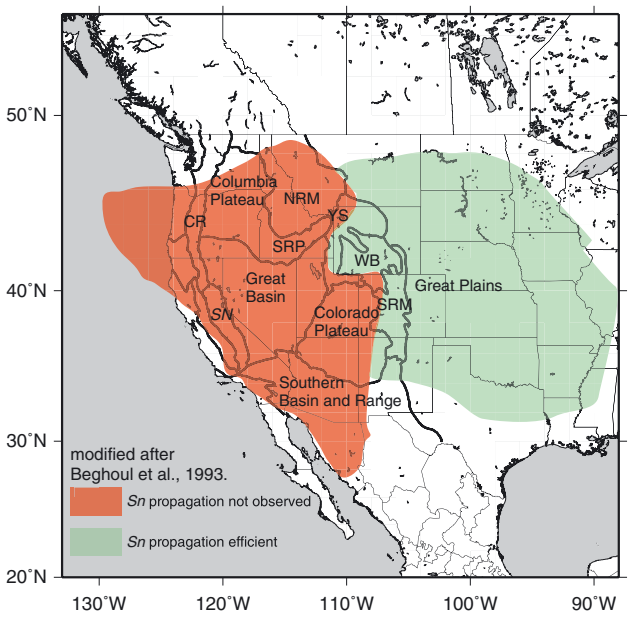

Figure 1. Map modified after *Beghoul et al.* [1993] showing that *Sn* is strongly attenuated for much of the Western United States but that clear *Sn* arrivals can be observed at stations in the Great Plains. The physiographic provinces are indicated by black lines and names. The abbreviations are in place for the Cascade Range (CR), Sierra Nevada (SN), Snake River Plain (SRP), Northern Rocky Mountains (NRM), Yellow Stone (YS), Wyoming Basin (WB), and Southern Rocky Mountains (SRM).

that the regions of *Sn* blockage are similar in scale to the velocity structures observed in the upper mantle.

[6] We apply stacking methods, similar to those employed locally in active source studies, on a regional scale using both earthquakes and quarry blasts, and measure the *Sn* amplitudes of these stacks at various locations. This allows us to map overall *Sn* propagation efficiency over large regions and image highly attenuating regions but without the need to inspect individual seismograms or the complications of formal attenuation modeling. We find evidence in our stacks for transmission of *Sn* below the northwestern portion of the Colorado Plateau, and in the center of the Great Basin, areas that coincide with regions of higher seismic velocities. As expected, we find *Sn* to be highly attenuated in the belt associated with recent volcanism and high heat flow that surrounds the central portion of the Great Basin and includes the Cascades back-arc, the Snake River Plain, and the southwestern margin of the Colorado Plateau.

2. Methods

[7] *Sn* is often emergent, buried by *P* wave coda, and hard to see by eye in individual seismograms. Stacking methods can greatly enhance such weak arrivals [e.g., *Richards-Dinger and Shearer*, 1997]. Common midpoint stacks are typically applied in seismic reflection experiments, but a similar approach can be used with refracted arrivals to obtain information on average seismic properties within a certain region [*Behm et al.*, 2007]. Here we stack seismograms that have the midpoint of their ray paths within a common two-dimensional cell. We then measure *Sn* amplitudes in these stacks to investigate variations in propagation efficiency or blockage at the various locations of the common midpoint cells.

[8] We downloaded waveforms from the ANF for about 8000 earthquakes and quarry blasts for broadband channels that have at least 10 *Pn* or *Sn* picks remaining after applying a similar space-time windowing procedure to that described in *Buehler and Shearer* [2010]. The ray paths for the stacks span ranges from 1.8° to 12°. We did not remove the instrument response since all the USArray transportable array stations are equipped with very similar instruments. We rotate the raw horizontal velocity seismograms into radial and transverse components using the epicenter location provided by the ANF and filter the waveforms between 0.8 and 4 Hz to remove microseisms and high-frequency noise.

[9] We proceed in similar fashion to that described in *Behm et al.* [2007]: We shift an equal area square cell with a width of 1.6° in increments of 0.8° across the Western United States. At each location, we find the event and station combinations that have their range midpoint within the window. Figure 2 shows an example for a common midpoint cell in the Great Basin. We stack all traces that satisfy this condition and that have a minimum signal-to-noise ratio of 2.5 for the first-arriving *Pn* phase on the vertical component. Since we cannot expect waveform coherency for the earthquakes from various ranges and azimuths around the common midpoint cell we find that stacking the short-term average to long-term average (STA/LTA) function of the waveforms works well [*Astiz et al.*, 1996]. We use 1 and 10 s for the short- and long-term windows, respectively. For stacking we use 0.25° for the range bin size and 0.5 s for the time bins (see supporting information).

[10] Similar to *Behm et al.* [2007], we find that the traces collected in individual distance bins stack with greater coherency if we align the *Sn* arrivals by means of a reduction velocity. For each stack, we find the average uppermost mantle *Pn* velocity and crustal thickness from our tomography [*Buehler and Shearer*, 2010] within the common midpoint cell. From this information we estimate an average slowness and intercept time for *Sn* at that location, assuming constant crustal velocity and Vp/Vs in the uppermost mantle. We then adjust the timing of the seismograms according to these parameters, in order for *Sn* to align at approximately zero time. We found that a more sophisticated approach with individual station and event time terms does not increase coherency and that the 0.5 s time bins are large enough to counteract small misalignments.

[11] Working with STA/LTA functions of seismograms is convenient, as the process functions as automatic gain control and often nicely enhances the appearance of individual phases. However, the shape of the waveforms is not conserved, and STA/LTA functions might bias the results, as more impulsive arrivals could map into a higher amplitude in the stacks. Therefore, we also produce common midpoint stacks using the envelope function of the seismograms for comparison (Figure 2b). We then use both the STA/LTA and the envelope stacks to measure the *Sn* amplitude. To properly capture the *Sn* signal strength we measure the mean amplitudes in a 10 s window that starts 4 s before the estimated *Sn* arrival time for the bins between a range of 3.25° and 4°. At certain locations *Sn* appears stronger at greater ranges, so we therefore also shift the amplitude-measuring window along the range axis in 0.25° increments and

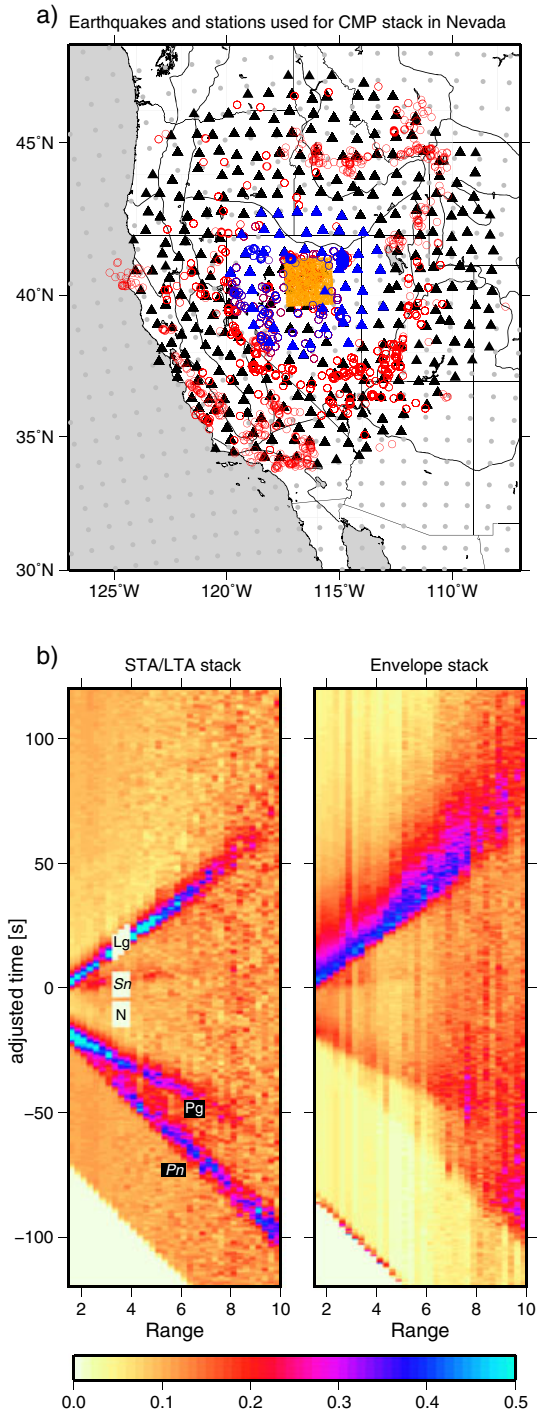

Figure 2. Common midpoint radial component stack examples for a location in central Nevada. (a) The stations (triangles) and events (circles) used to image wave propagation within the orange square. The blue triangles and circles indicate stations and events that contribute to the stack between a range of 3.25–4.0° where we measure the amplitudes. (b) STA/LTA and envelope stacks showing the characteristics of the regional phases for this region. The windows that we use to measure the *Sn*, Lg, and noise amplitudes are indicated by the light yellow polygons. Individual traces of the stacks are normalized by their maximum amplitudes, and each range bin stack is normalized by the number of traces in that bin. The color scale is capped at 0.5 for visual enhancement of weaker phases.

measure the maximum signal at any range between 3.25° and 8°. This reduces the localization and makes interpretation more difficult but indicates the general visibility of *Sn* in a stack more clearly. Often *Sn* appears stronger at shorter ranges, but here we risk that the *Sn* phase amplitude is contaminated by energy of crustal Lg. However, since energy transfer between *Sn* and the crustal phase can occur, especially at continental margins [*Isacks and Stephens*, 1975] and possibly continental plateaus, we separately measure the mean amplitude of Lg using a similar window. We normalize both the measured *Sn* and Lg amplitudes with the mean amplitude of a window in the *P* coda.

[12] This simple waveform-stacking approach is unable to return high-resolution attenuation images as for example produced by *Phillips and Stead* [2008] for USArray Lg. Attenuation tomography for *Sn* is difficult since the phase is generally only well approximated as a head wave that travels horizontally right below the Moho at short ranges [e.g., *Sereno*, 1989]. At longer ranges, *Pn* and *Sn* generally evolve into turning waves and modeling them as pure head waves with a horizontal uppermost mantle path will introduce errors. The ranges over which this transition occurs depend on the velocity gradient in the mantle lid and on the crustal thickness [*Sereno*, 1989]. The type of head wave that is observed up to teleseismic distances is typically described as a sum of whispering gallery or interference waves which travel in the mantle lid between the Moho and the low-velocity zone of the upper mantle [e.g., *Menke and Richards*, 1980]. Attenuation behavior of such waves is generally quite complicated and different from the behavior of pure head waves, and the amplitudes will depend on the velocity gradient in the uppermost mantle [*Hill*, 1973; *Braile and Smith*, 1975]. Because of these complications, we do not attempt to formally model the *Sn* attenuation but try to determine the broad variations of the propagation efficiency. The method we apply allows us to process a large number of seismic observations from USArray and improves our view of *Sn* propagation efficiency in the Western United States.

3. Results

[13] Figure 3 displays the measured stack amplitudes, and Figure 4 shows corresponding stacks for various locations for the transverse components. Images for the radial component are not displayed but look similar. The results from the STA/LTA and envelope stacks show similar features although the structures in the envelope map are less distinct (compare Figure 3a with Figure 3c). This is to be expected as the STA/LTA filter is more sensitive to changes in the shape and amplitude of the signal. Note that strong *P* arrivals are visible on the transverse component as a result of this filter sensitivity. Measuring amplitudes with just one range window at 3.25° and 4° seems to capture the characteristics of the stacks well, except for a few regions, as for example north of the Colorado Plateau, where *Sn* is visible more clearly at larger distances (Figure 3b).

[14] Similar to observations of seismic velocities, the *Sn* amplitude structure is quite heterogeneous. As in *Rodgers et al.* [1997], the measured *Sn* amplitudes are typically lower in regions of low *Pn* velocities. We find the most distinctive zone without evidence for *Sn* propagation in the back-arc of the Cascade Range, a region with recent volcanism.

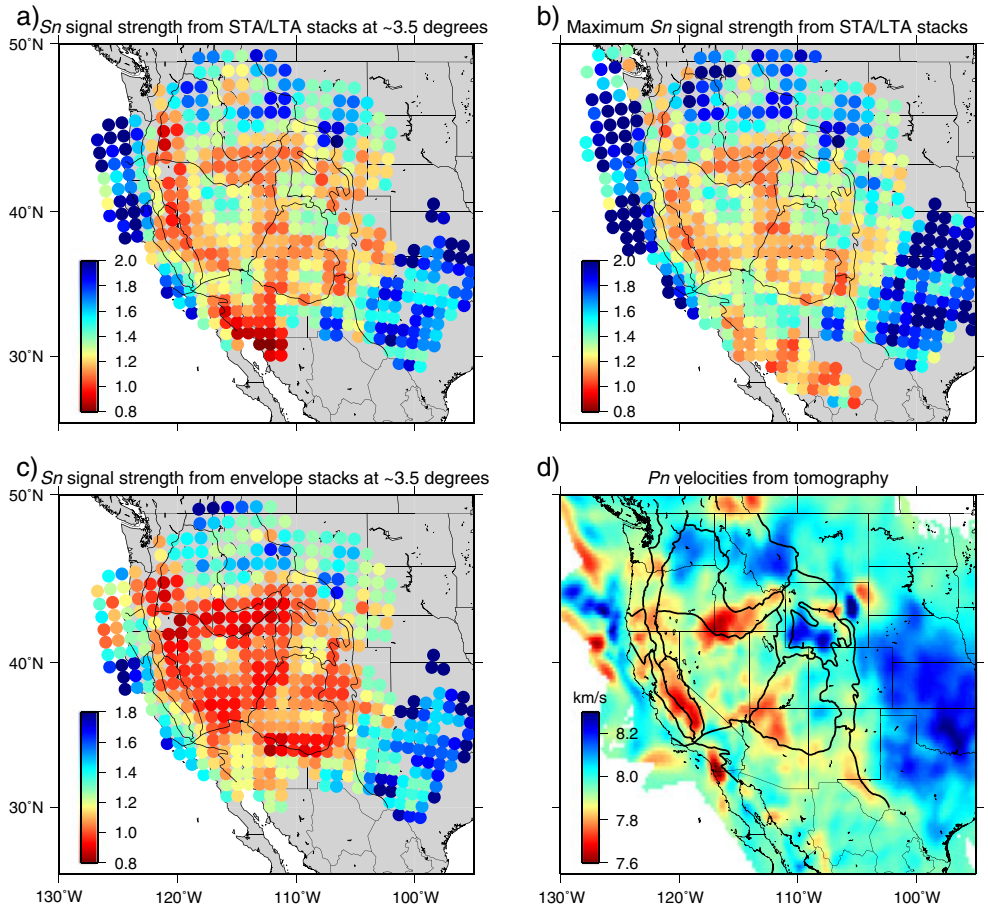

Figure 3. (a) Measured *Sn* amplitudes at a range of 3.25 to 4° in STA/LTA stacks normalized by the mean amplitude of the *P* coda. Blue colors indicate regions of strong *Sn* signal; red colors show regions that greatly attenuate *Sn*. Regions without colored circles do not have enough data after processing. (b) same as Figure 3a, but the maximum amplitudes of all range windows are plotted. (c) Measured *Sn* amplitudes at a range of 3.25 to 4° in envelope stacks normalized by the mean amplitude of the *P* coda. (d) *Pn* velocities from tomography for comparison. Measured *Sn* amplitudes are typically lower in regions of low *Pn* velocities.

Similarly, we do not observe *Sn* in stacks across the Snake River Plain and the current location of the Yellowstone hotspot, regions of low *Pn* velocities (Figure 3d, updated model from *Buehler and Shearer* [2010]) and very low shear velocities [*Schmandt and Humphreys*, 2010]. These observations could indicate zones of partial melt in the uppermost mantle. To the north of the Snake River Plain and Yellowstone the character of the stacks changes abruptly and *Sn* is clearly visible in the stacks. We also find clear *Sn* arrivals in the region of the Columbia Plateau, where recent receiver function analysis showed a local increase in the depth of the lithosphere-asthenosphere boundary [*Kumar et al.*, 2012].

[15] We do not observe *Sn* in the transition zone between the Great Basin and the Colorado Plateau. The Basin and Range Province is associated with high heat flow [e.g., *Lachenbruch*, 1978] that is generally related to strong *Sn* attenuation [*Molnar and Oliver*, 1969]. Yet interestingly we see a region of *Sn* propagation in the center of the Great Basin, in the broad region of a previously imaged higher-velocity body interpreted as a lithospheric drip [*West et al.*, 2009], and close to the low heat flow anomaly in south-central Nevada [*Lachenbruch*, 1978]. *West et al.* [2009] explain that the downwelling would locally increase the thickness of the lithosphere and potentially reduce its thickness around the periphery of the Great Basin. It is a current understanding that the mantle lid of lithosphere needs to be sufficiently thick in order for *Sn* to propagate. However, at the relatively short epicentral distances over which we measure the amplitudes the phase should propagate near the top of the mantle similar to a pure head wave. Still, the stacks show a clear *Sn* strand to a range of about 6° (Figure 4, stack 3) before the phase fades, supporting the existence of a locally colder and possibly thicker lithosphere.

[16] The previous study by *Beghoul et al.* [1993] showed that *Sn* does not propagate across the Colorado Plateau. They argued that the absence of *Sn* indicates a thin mantle lid since the *Pn* velocities below the central Colorado Plateau are relatively high, and therefore, *Sn* attenuation is likely not caused by thermal effects. Their study used WWSSN stations, and the ray paths were between 3 and 16°. Since the station network was much sparser pre-USArray, many of the *Sn* paths analyzed traveled across the entire Colorado Plateau. In our study, we observe *Sn* at shorter ranges for some parts of the Colorado Plateau, and the strength of the amplitudes in the stacks change from the northeastern section to the southwestern part. Our stacks that sample the southwestern

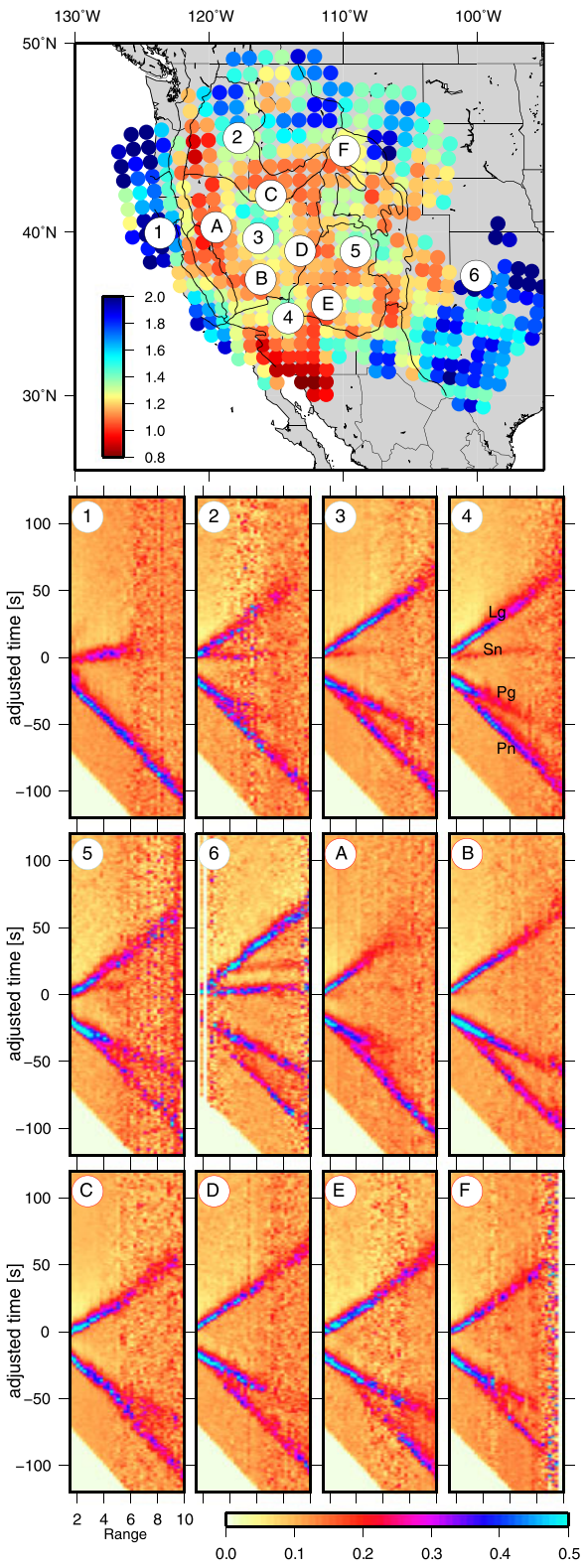

Figure 4. Images of individual STA/LTA common midpoint transverse component stacks at various locations. Number or letter in the top left corner of each stack corresponds to the number/letter in the map on the top. Stacks 1–6 show *Sn*, but *Sn* is attenuated in stacks A–F.

part of the Plateau do not show evidence for *Sn*, roughly for the same area as USArray uppermost mantle tomographies show low shear velocities. However, stacks from ray paths that mostly sample the northeastern part of the Colorado Plateau, generally associated with faster upper mantle velocities, show a low-energy *Sn* strand arriving slightly later than the time estimated from the *Pn* Moho depth model (Figure 4, stack 5). This suggests that *Sn* is strongly attenuated when it travels across the likely warmer western and southern margins of the Colorado Plateau, where *Schmandt and Humphreys* [2010] show very low shear velocities at 90 km depth, and that a thin lithosphere is not necessarily the primary reason for *Sn* attenuation. This is in agreement with recent mapping of the asthenosphere-lithosphere boundary (LAB) below the Western United States with receiver functions [*Kumar et al.*, 2012; *Levander and Miller*, 2012], which generally show a thicker lithosphere below the Colorado Plateau compared to the adjacent Basin and Range Province. *Kumar et al.* [2012] find boundary depths up to 140 km below the Colorado Plateau. The estimates by *Levander and Miller* [2012] are lower at ∼90 km but still significantly deeper compared to their measured LAB depth of ∼65 km below the Basin and Range. In addition, *Obrebski et al.* [2011] noted that their observation of high shear velocities might be consistent with a stable and relatively thick lithosphere for the northeastern part of the Colorado Plateau.

[17] Compared to the heterogeneous picture of *Sn* attenuation, the amplitude of the crustal shear wave changes more gradually over the Western United States (Figure 5). It is recognized that Lg does not traverse across oceanic crust [e.g., *Kennett and Furumura*, 2001], and we do not observe Sg or Lg in stacks at the western coast with contributions from mostly offshore earthquakes. *Phillips and Stead* [2008] also show strong Lg attenuation along the western margin. *Isacks and Stephens* [1975] describe the conversion of *Sn* to Lg at continental margins, and we observe that the Lg amplitude gradually increases away from the coast to a maximum in the central Great Basin around 115°W. But more detailed work would be needed to assess conversions of the phases.

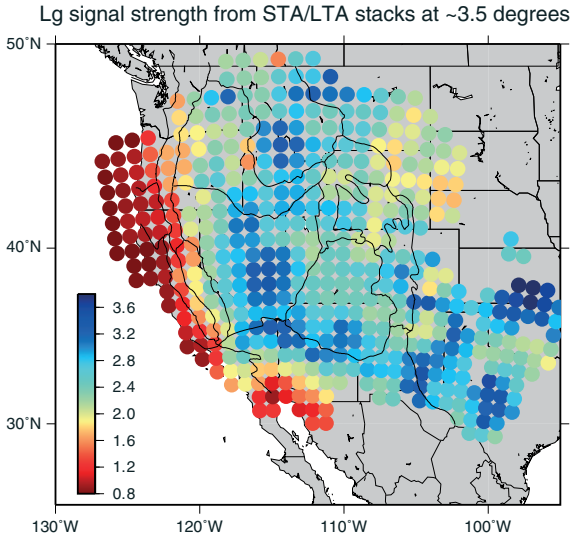

Figure 5. Measured Lg amplitudes in STA/LTA stacks normalized by the mean amplitude of the *P* coda.

In addition, we do not find anomalous Lg amplitudes for the Colorado Plateau that would suggest any significant energy transfer from the uppermost mantle into the crust. Similar to *Phillips and Stead* [2008],we observe that Lg, in contrast to *Sn*, generally propagates well in the Snake River Plain.

4. Summary

[18] We examine the propagation of *Sn* in the Western United States. The dense USArray station coverage allows us to experiment with methods that are conventionally used in active source studies at local scales. Common midpoint stacking analysis shows that *Sn* is highly attenuated across smaller and more localized regions than previously assumed, mostly where the paths cross the perimeter of the Great Basin. We find that the regions with high *Sn* attenuation correlate with volcanism and previously imaged low-velocity anomalies in the uppermost mantle. These observations are in agreement with local zones of partially molten uppermost mantle material. We find *Sn* arrivals along the coast of California, Oregon, and Washington, in the central Great Basin, in the northeastern part of the Colorado Plateau, and the Columbia Plateau. The structure of the *Sn* propagation efficiency below the Colorado Plateau is nonuniform, and the signal strength increases from southwest to northeast. This is in agreement with a potentially intact and thicker lithosphere in the northeastern part of the Colorado Plateau, as previously suggested as an explanation for the higher body wave velocities in this region, but more localized measurements are needed for more conclusive interpretations.

[19] **Acknowledgments.** We thank Luciana Astiz for discussions and assistance with the Antelope system and Tom Hearn and two anonymous reviewers for their constructive comments. This research was supported by grant EAR-0950391 from the National Science Foundation.

[20] The Editor thanks Thomas Hearn and an anonymous reviewer for their assistance in reviewing this paper.

References

Astiz, L., P. Earle, and P. Shearer (1996), Global stacking of broadband seismograms, *Seismol. Res. Lett.*, *67*(4), 8–18, doi:10.1785/gssrl.67.4.8.

Barron, J., and K. Priestley (2009), Observations of frequency-dependent Sn propagation in Northern Tibet, *Geophys. J. Int.*, *179*(1), 475–488.

Beghoul, N., M. Barazangi, and B. L. Isacks (1993), Lithospheric structure of Tibet and western North America: Mechanisms of uplift and a comparative study, *J. Geophys. Res.*, *98*(B2), 1997–2016.

Behm, M., E. Brkl, W. Chwatal, and H. Thybo (2007), Application of stacking and inversion techniques to three-dimensional wide-angle reflection and refraction seismic data of the Eastern Alps, *Geophys. J. Int.*, *170*(1), 275–298, doi:10.1111/j.1365-246X.2007.03393.x.

Braile, L. W., and R. B. Smith (1975), Guide to the interpretation of crustal refraction profiles, *Geophys. J. Int.*, *40*(2), 145–176.

Buehler, J. S., and P. M. Shearer (2010), Pn tomography of the western United States using USArray, *J. Geophys. Res.*, *115*, B09315, doi:10.1029/2009JB006874.

Calvert, A., E. Sandvol, D. Seber, M. Barazangi, F. Vidal, G. Alguacil, and N. Jabour (2000), Propagation of regional seismic phases (Lg and Sn) and Pn velocity structure along the Africa Iberia plate boundary zone: Tectonic implications, *Geophys. J. Int.*, *142*(2), 384–408.

Diaz, J., A. Gil, and J. Gallart (2013), Uppermost mantle seismic velocity and anisotropy in the Euro-Mediterranean region from Pn and Sn tomography, *Geophys. J. Int.*, *192*(1), 310–325, doi:10.1093/gji/ggs016.

Goek, R., E. Sandvol, N. Tkelli, D. Seber, and M. Barazangi (2003), Sn attenuation in the Anatolian and Iranian plateau and surrounding regions, *Geophys. Res. Lett.*, *30*(24), 8042, doi:10.1029/2003GL018020.

Goes, S., and S. van der Lee (2002), Thermal structure of the North American uppermost mantle inferred from seismic tomography, *J. Geophys. Res.*, *107*(B3), ETG 2-1–ETG 2-13, doi:10.1029/2000JB000049.

Hill, D. P. (1973), Critically refracted waves in a spherically symmetric radially heterogeneous earth model, *Geophys. J. Int.*, *34*(2), 149–177.

Isacks, B. L., and C. Stephens (1975), Conversion of Sn to Lg at a continental margin, *Bull. Seismol. Soc. Am.*, *65*(1), 235–244.

Kennett, B. L. N., and T. Furumura (2001), Regional phases in continental and oceanic environments, *Geophys. J. Int.*, *146* (2), 562–568, doi:10.1046/j.1365-246x.2001.01467.x.

Kumar, P., X. Yuan, R. Kind, and J. Mechie (2012), The lithosphere-asthenosphere boundary observed with USArray receiver functions, *Solid Earth*, *3*, 149–159.

Lachenbruch, A. (1978), Heat flow in the Basin and Range province and thermal effects of tectonic extension, *Pure Appl. Geophys.*, *117*(1-2), 34–50.

Levander, A., and M. S. Miller (2012), Evolutionary aspects of lithosphere discontinuity structure in the western U.S, *Geochem. Geophys. Geosyst.*, *13*, Q0AK07, doi:10.1029/2012GC004056.

Levander, A., B. Schmandt, M. S. Miller, K. Liu, K. E. Karlstrom, R. S. Crow, C.-T. A. Lee, and E. D. Humphreys (2011), Continuing Colorado plateau uplift by delamination-style convective lithospheric downwelling, *Nature*, *472*(7344), 461–465.

Lin, F.-C., M. H. Ritzwoller, Y. Yang, M. P. Moschetti, and M. J. Fouch (2011), Complex and variable crustal and uppermost mantle seismic anisotropy in the western United States, *Nat. Geosci.*, *4*(1), 55–61.

Menke, W. H., and P. G. Richards (1980), Crust–mantle whispering gallery phases: A deterministic model of teleseismic Pn wave propagation, *J. Geophys. Res.*, *85*(B10), 5416–5422.

Molnar, P., and J. Oliver (1969), Lateral variations of attenuation in the upper mantle and discontinuities in the lithosphere, *J. Geophys. Res.*, *74*(10), 2648–2682.

Ni, J., and M. Barazangi (1983), High-frequency seismic wave propagation beneath the Indian Shield, Himalayan Arc, Tibetan Plateau and surrounding regions: High uppermost mantle velocities and efficient Sn propagation beneath Tibet, *Geophys. J. R. Astron. Soc.*, *72*(3), 665–689.

Obrebski, M., R. M. Allen, F. Pollitz, and S.-H. Hung (2011), Lithosphere-asthenosphere interaction beneath the western United States from the joint inversion of body-wave travel times and surface-wave phase velocities, *Geophys. J. Int.*, *185*(2), 1003–1021.

Pei, S., J. Zhao, Y. Sun, Z. Xu, S. Wang, H. Liu, C. A. Rowe, M. N. Toksz, and X. Gao (2007), Upper mantle seismic velocities and anisotropy in China determined through Pn and Sn tomography, *J. Geophys. Res.*, *112*, B05312, doi:10.1029/2006JB004409.

Phillips, W. S., and R. J. Stead (2008), Attenuation of Lg in the western US using the USArray, *Geophys. Res. Lett.*, *35*, L07307, doi:10.1029/2007GL032926.

Richards-Dinger, K. B., and P. M. Shearer (1997), Estimating crustal thickness in southern California by stacking PmP arrivals, *J. Geophys. Res.*, *102*(B7), 15,211–15,224.

Rodgers, A. J., J. F. Ni, and T. M. Hearn (1997), Propagation characteristics of short-period Sn and Lg in the Middle East, *Bull. Seismol. Soc. Am.*, *87*(2), 396–413.

Schmandt, B., and E. Humphreys (2010), Complex subduction and small-scale convection revealed by body-wave tomography of the western United States upper mantle, *Earth Planet. Sci. Lett.*, *297*, 435–445.

Sereno, T. J. (1989), Numerical modeling of Pn geometric spreading and empirically determined attenuation of Pn and Lg phases recorded in eastern Kazakhstan, *Tech. Rep.*, Science Applications International Corporation.

Stephens, C., and B. L. Isacks (1977), Toward an understanding of Sn: Normal modes of love waves in an oceanic structure, *Bull. Seismol. Soc. Am.*, *67*(1), 69–78.

West, J. D., M. J. Fouch, J. B. Roth, and L. T. Elkins-Tanton (2009), Vertical mantle flow associated with a lithospheric drip beneath the Great Basin, *Nat. Geosci.*, *2*(6), 439–444.